Journal of the American College of Cardiology
© 2010 by the American College of Cardiology Foundation
Published by Elsevier Inc.

Vol. 55, No. 20, 2010
ISSN 0735-1097/$36.00
doi:10.1016/j.jacc.2009.10.081

Differential Effects of Progenitor Cell Populations on Left Ventricular Remodeling and Myocardial Neovascularization After Myocardial Infarction

Christophe Dubois, MD,* Xiaoshun Liu, MD, PhD,‖ Piet Claus, PhD,* Glenn Marsboom, PhD,‖ Peter Pokreisz, PhD,‖ Sara Vandenwijngaert, MSc,‖ Hélène Dépelteau, MD,† Witold Streb, MD,* Lertlak Chaothawee, MD,† Frederik Maes, PhD,† Olivier Gheysens, MD, PhD,‡ Zeger Debyser, MD, PhD,¶ Hilde Gillijns, BSc,‖ Marijke Pellens, BSc,‖ Thierry Vandendriessche, PhD,‖ Marinee Chuah, PhD,‖ Desiré Collen, MD, PhD,‖ Erik Verbeken, MD, PhD,§ Ann Belmans, MSc,# Frans Van de Werf, MD, PhD,* Jan Bogaert, MD, PhD,† Stefan Janssens, MD, PhD*‖

Leuven, Belgium

Objectives We compared biological repair after acute myocardial infarction (AMI) with selected porcine progenitor cell populations.

Background Cell types and mechanisms responsible for myocardial repair after AMI remain uncertain.

Methods In a blinded, randomized study, we infused autologous late-outgrowth endothelial progenitor cells (EPC) ($n = 10$, $34 \pm 22 \times 10^6$ CD29-31-positive, capable of tube formation), allogeneic green fluorescent peptide–labeled mesenchymal stem cells (MSC) ($n = 11$, $10 \pm 2 \times 10^6$ CD29-44-90-positive, capable of adipogenic and osteogenic differentiation), or vehicle (CON) ($n = 12$) in the circumflex artery 1 week after AMI. Systolic function (ejection fraction), left ventricular (LV) end-diastolic and end-systolic volumes, and infarct size were assessed with magnetic resonance imaging at 1 week and 7 weeks. Cell engraftment and vascular density were evaluated on postmortem sections.

Results Recovery of LV ejection fraction from 1 to 7 weeks was similar between groups, but LV remodeling markedly differed with a greater increase of LV end-systolic volume in MSC and CON ($+11 \pm 12$ ml/m^2 and $+7 \pm 8$ ml/m^2 vs. -3 ± 11 ml/m^2 in EPC, respectively, $p = 0.04$), and a similar trend was noted for LV end-diastolic volume ($p = 0.09$). After EPC, infarct size decreased more in segments with >50% infarct transmurality ($p = 0.02$ vs. MSC and CON) and was associated with a greater vascular density ($p = 0.01$). Late outgrowth EPCs secrete higher levels of the pro-angiogenic placental growth factor (733 [277 to 1,214] pg/10^6 vs. 59 [34 to 88] pg/10^6 cells in MSC, $p = 0.03$) and incorporate in neovessels in vivo.

Conclusions Infusion of late-outgrowth EPCs after AMI improves myocardial infarction remodeling via enhanced neovascularization but does not mediate cardiomyogenesis. Endothelial progenitor cell transfer might hold promise for heart failure prevention via pro-angiogenic or paracrine matrix-modulating effects. (J Am Coll Cardiol 2010;55:2232–43) © 2010 by the American College of Cardiology Foundation

Cardiac cell transfer is a promising new strategy for biological repair of the dysfunctional heart. Clinical translation of initial proof of concept studies with bone marrow-derived mononuclear progenitor cells in mice (1) has gained significant momentum, but studies in patients with acute myocardial infarction (AMI) have shown mixed results (2–4). In

From the *Division of Cardiology, Department of Cardiovascular Diseases, and the Departments of †Radiology, ‡Nuclear Medicine, and §Medical Diagnostic Sciences, Gasthuisberg University Hospitals Leuven, Leuven, Belgium; ‖Vesalius Research Center, Flanders Institute for Biotechnology (VIB); and the Departments of ¶Molecular Medicine and #Public Health, Biostatistical Center, KU-Leuven, Leuven, Belgium. This work was supported by grants of the Fund for Scientific Research–Flanders G.0442.06 and G.0280.05, VIB (Dr. Janssens) and the Research Fund KU-Leuven GOA/2007/13 (Drs. Janssens and Pokreisz). Dr. Janssens is holder of a chair supported by AstraZeneca. Dr. Dépelteau was supported by a fellowship, funded by the Royal College of Physicians and Surgeons of Canada.

Manuscript received May 29, 2009; revised manuscript received October 5, 2009, accepted October 5, 2009.

most randomized studies a heterogeneous mononuclear cell (MNC) population was infused in the infarct-related coronary artery (IRA), and change in global ejection fraction was evaluated as a surrogate primary efficacy end point.

See page 2254

There is a growing recognition that indirect paracrine trophic effects rather than cardiomyogenesis resulting from progenitor cell transdifferentiation mediate the observed changes in contractile function or infarct size after infusion of a mixed MNC population (5). Although critically important variables, including doses and delivery routes of labeled mixed mononuclear or mesenchymal (MSC) progenitor cells, have been investigated in representative large animal models (6–10), direct comparison of selected cell populations has received limited attention. Therefore we compared functional and structural recovery after AMI in pigs after intracoronary (IC) infusion of autologous late outgrowth endothelial progenitor cells (EPCs) versus allogeneic MSCs.

Methods

Study design. The Animal Care and Use Committee of University of Leuven approved this study. At 1 week after AMI, pigs were randomly assigned to blinded IC delivery of control medium (CON), autologous EPCs, or allogeneic MSCs. Hemodynamic variables were measured at baseline and after 1 week and 7 weeks. Magnetic resonance imaging (MRI) was performed at 1 week and 7 weeks after AMI in a subgroup of pigs. All pigs were killed at 7 weeks. Growth-related changes in myocardial mass and volumes were evaluated in a separate series of healthy pigs over the same time period.

Cell preparation. ISOLATION AND CULTURE OF AUTOLOGOUS LATE-OUTGROWTH EPCs. Mononuclear cells were isolated from 40 ml blood by Lymphoprep density centrifugation (Axis-Shield, Oslo, Norway) and 50 to 100 $\times$ 10^6 MNCs were plated on fibronectin-coated (5 μg/ml) dishes in EBM2 (Clonetics, San Diego, California), supplemented with 5% FBS (Invitrogen, Carlsbad, California), vascular endothelial growth factor, human epidermal growth factor, human basic fibroblast growth factor, ascorbic acid, R3-insulin-like growth factor-1, and gentamycin/amphotericin-B. After 4 days, nonadherent cells were removed and cells were cultured for an additional 3 weeks. Late-outgrowth EPCs were then incubated for 24 h with iron oxide (Endorem, Guerbet, France) and poly-L-lysine (Sigma) and diluted in phosphate-buffered saline for phenotypic characterization and IC delivery. Alternatively, for biodistribution studies, EPCs were genetically labeled with a lentiviral reporter construct (p24 titer 5.5 $\times$ 10^6 pg/ml, 1/150 dilution) expressing nuclear targeted beta-galactosidase (LacZ). Expression of surface markers was performed by immunofluorescence and flow cytometry (CD31, CD45, CD29, and SLA DR).

ISOLATION AND CULTURE OF ALLOGENEIC MSCs. Bone marrow was aspirated from the femur (10 ml), diluted in phosphate-buffered saline, 1:3, and filtered. The MNC fraction was isolated with Lymphoprep (Axis-Shield) and amplified in adherent cell cultures (0.1% gelatine-coating). Phenotypic characterization of MSCs was performed by evaluating expression of surface markers (CD31, CD90, CD29, CD44, and CD45), and plasticity was confirmed with adipogenic and osteogenic differentiation (stem cell technology) (11,12). The MSCs were genetically labeled with lentiviral vectors encoding enhanced green fluorescent peptide (GFP) or nuclear targeted LacZ gene for biodistribution studies. The functional titer of the GFP-expressing lentiviral vector was 1.75 $\times$ 10^7 U/ml; multiplicity of infection was 14.

Induction of AMI and hemodynamic measurements. Pigs (20 to 30 kg) were pre-treated with 400 mg amiodarone for 1 week and with aspirin and clopidogrel 1 day before AMI. Pigs were pre-anesthetized with ketamine hydrochloride (20 mg/kg, IM) (Anesketin, Eurovet, Heusden, Belgium), followed by continuous infusion of propofol (0.15 mg/kg/min, IV), intubated and ventilated with a 1:1 mixture of air and oxygen and anticoagulated (10,000 IU heparin). The AMI was induced under continuous electrocardiographic (ECG) monitoring by stenting and 90-min balloon occlusion of the proximal circumflex artery, followed by reperfusion. One week later, control medium, EPC, or MSC were injected via a perfusion catheter inflated in the stented circumflex artery segment during a 10-min stop-flow condition. Immediately after cell transfer and before pigs were killed, angiography of the IRA was repeated to confirm patency. Aspirin (100 mg) and clopidogrel (75 mg) were given daily for 7 weeks.

Hemodynamic variables were measured with a 7-F Millar catheter positioned in the left ventricle (LV). Heart rate, LV systolic and diastolic pressures, and first derivatives thereof ($dP/dt_{max/min}$) were recorded at baseline, before cell transfer,

Abbreviations and Acronyms

AMI = acute myocardial infarction
CON = vehicle, control medium
ECG = electrocardiographic
EDV = end-diastolic volume
EPC = endothelial progenitor cell
ESV = end-systolic volume
GFP = green fluorescent peptide
IC = intracoronary
IGF = insulin-like growth factor
IRA = infarct related artery
LacZ = beta-galactosidase
LV = left ventricle/ventricular
LVEDV = left ventricular end-diastolic volume
LVESV = left ventricular end-systolic volume
MMP = matrix metalloproteinase
MNC = mononuclear cell
MRI = magnetic resonance imaging
MSC = mesenchymal stem cell
PLGF = placental growth factor
qPCR = quantitative polymerase chain reaction
TGF = transforming growth factor
TTC = 2,3,5-triphenyltetrazoliumchloride
VEGF = vascular endothelial growth factor

and before pigs were killed and processed with Powerlab software (AD Instruments, Oxfordshire, United Kingdom).

MRI: cine-angiography, delayed enhancement infarct, and perfusion studies. Cardiac MRI (1.5-T, Sonata, Siemens, Erlangen, Germany) was performed at 1 week and 7 weeks after AMI. All studies were done with Siemens Numaris-4 software, ECG triggering, and cardiac-dedicated surface coils. Global function was assessed with breath-hold cine MRI in short axis, vertical axis, and horizontal long axis. In short axis, the LV was completely encompassed by contiguous 6-mm-thick slices. Infarct area was defined as the zone of bright signal on late-enhanced images (i.e., 10 to 20 min after injection of 0.15 mmol/kg of gadopentetate dimeglumine), with an inversion-recovery gradient-echo technique. All MRI studies with assessment of global LV function (left ventricular end-diastolic volume [LVEDV] and left ventricular end-systolic volume [LVESV]) and calculation of infarct volume were analyzed on an offline workstation (ARGUS, Siemens) by investigators unaware of treatment allocation (2). We used the 16 segments model to grade transmural extent of late hyperenhancement and reported transmurality estimates at 7-week follow-up for segments with a mean baseline hyperenhancement of 10%, 25%, 50%, 75%, and 90% (13,14). First-pass perfusion imaging after bolus injections of gadopentetate dimeglumine (0.05 mmol/kg, 3.5 cc/s) was performed for 1 min, obtaining 80 measurements (0.8 s temporal resolution) with ECG-gated steady state free precession imaging pulse sequence in short-axis direction. Relative upslope was calculated for segments 5-6-11-12, reflecting the circumflex artery perfusion area (15,16).

Immunohistochemical, reverse-transcription polymerase chain reaction analysis of myocardial biopsies, and molecular profiling of progenitor cells. At week 7, biopsies were taken from 1-cm-thick transverse sections from infarct core, border zone, and remote areas and stored in 10% formalin or flash frozen in liquid nitrogen. Adjacent myocardial transsections were stained with 1% 2,3,5-triphenyltetrazoliumchloride (TTC) for 10 min to delineate infarct borders. The GFP and Prussian blue stainings were performed to detect labeled MSCs and EPCs, respectively. To confirm GFP expression, 10- to 30-μm frozen sections were analyzed with dual photon laser microscopy equipped with spectral analysis detector (Zeiss LSM 510 Meta, Carl Zeiss, Oberkochen, Germany). Isolated GFP-infected bone marrow cells served as positive control. Vascular density was blindly assessed on 5-μm-thick sections by counting Isolectin-B4-stained (L5391, Sigma) vessels in 5 high-power fields in infarct core and border zones and in remote myocardium in 9 pigs/group. We blindly investigated the presence of dense (Type I) and loosely assembled (Type III) collagen with circularly polarized light on randomly selected Sirius red-stained sections from the infarct border zone of CON, EPC, and MSC. Expression of genes involved in LV remodeling, neovascularization, and apoptosis was measured with quantitative polymerase chain reaction (qPCR) in extracts from these areas (Online Table 1).

In addition, we studied LacZ-labeled EPC and MSC engraftment and survival in the infarcted myocardium at 7 weeks and biodistribution to remote organs at 1 week. Different zones in the heart, lung, liver, kidney, spleen, and

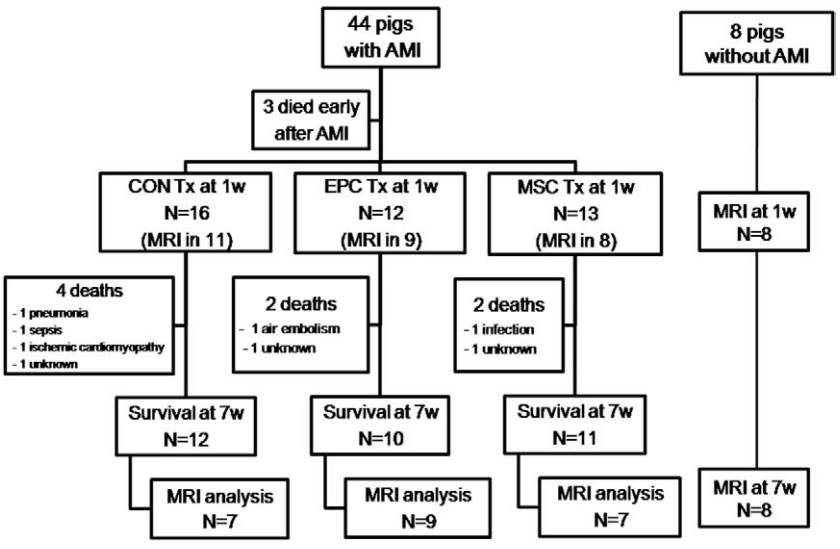

Figure 1 Schematic Presentation of Study Flow

Of a total of 44 infarcted pigs, 41 underwent cell transfer at 1 week, and 33 survived at 7 weeks; 23 pigs underwent serial magnetic resonance imaging (MRI). Growth-related changes in myocardial mass and volumes were evaluated in 8 healthy pigs. AMI = acute myocardial infarction; CON = vehicle; EPC = endothelial progenitor cell; MSC = mesenchymal stem cell; Tx = transfer.

brain were sampled for histochemical LacZ staining and qPCR analysis of labeled cells.

Transcript levels of genes encoding growth factors were analyzed in 3 independent cultures of EPCs and MSCs, whereas secretome in conditioned medium from cultured EPCs and MSCs was analyzed in 4 independent experiments with enzyme-linked immunoadsorbent assay for fibroblast growth factor-2, vascular endothelial growth factor (VEGF), insulin-like growth factor (IGF)-1, transforming growth factor beta-1 (R&D Systems, Minneapolis, Minnesota), and placental growth factor (PLGF) (Thrombogenics, Leuven, Belgium).

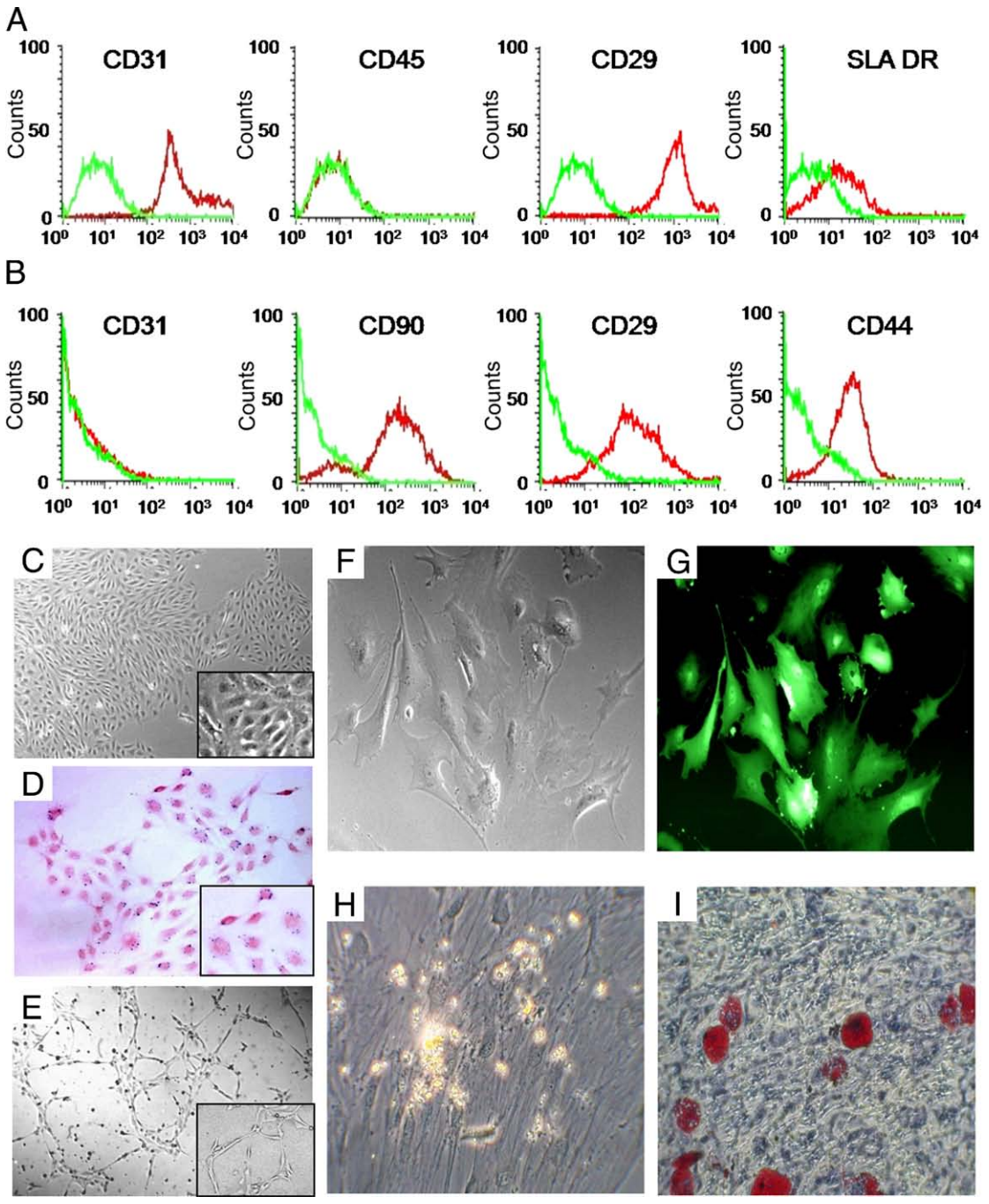

Figure 2 **Phenotypic Analysis and Labeling of Progenitor Cells In Vitro**

Flow cytometry of EPC and MSC **(A, B)** and representative examples of culture-expanded autologous unlabeled **(C)** and Endorem-labeled EPCs **(D)** and allogeneic MSCs are shown **(F, G)**. Progenitor cell function was confirmed by tube formation on matrigel **(E)**. The MSCs **(F)** were green fluorescent peptide-labeled **(G)**, and plasticity was confirmed by osteogenic differentiation on Alizarin stain **(H)** and adipogenic differentiation on oil-red stain **(I)**. Abbreviations as in Figure 1.

JACC Vol. 55, No. 20, 2010
May 18, 2010:2232–43

Statistical analysis. Hemodynamic and MRI data and vascular density are presented as mean and SD, and changes from baseline to 7 weeks were analyzed with Kruskal-Wallis tests. Transcriptome and secretome data in EPC and MSC are presented as median, minimum, and maximum and compared with Mann-Whitney *U* tests. Differences in matrix gene expression and vascular density between treatment groups were analyzed with Kruskal-Wallis tests. Relative upslope in circumflex artery perfused segments and infarct transmurality were compared with analysis of variance for repeated measures. In this model, we adjusted for possible correlations among all segments by taking into account the distance between 2 segments. We assumed that these correlations decreased exponentially as the distance increased between the segments. All treatment differences were estimated and presented with 95% confidence intervals. To account for multiple pairwise comparisons between treatment groups, significance level was adjusted with Tukey's method. All statistical tests were 2-sided and assessed at the 5% significance level. All analyses were performed with SAS (version 9.2, SAS Institute, Cary, North Carolina).

Results

Study group. Of 52 pigs, we infarcted 44 pigs and completed invasive hemodynamic assessment at 7 weeks in 33 animals (12 CON, 10 EPC, 11 MSC) (Fig. 1). Of these, 23 (7 CON, 9 EPC, 7 MSC) underwent serial MRI. Three pigs died during induction of AMI (before allocation), whereas after allocation 4 died in CON (1 pneumonia, 1 sepsis, 1 ischemic cardiomyopathy, and 1 unknown), 2 died in EPC (1 air embolism during cell transfer, 1 unknown), and 2 died in MSC (1 infection, 1 unknown). Eight additional pigs were serially scanned at 1 week and 7 weeks to account for growth- and biological age-related changes in LV volumes and mass.

Phenotypic and functional analysis of labeled porcine progenitor cells. Flow cytometry of EPCs revealed uniform expression of CD29 and CD31 but not the monocytic marker CD45, whereas MSCs expressed CD29, CD44, and CD90 (Fig. 2). The MSCs displayed a typical spindle-shape appearance with a >80% transfection efficiency for GFP and retained plasticity after multiple passages and labeling (Figs. 2H and 2I). Late outgrowth EPCs induced vascular network formation on matrigel (Fig. 2E).

Transcriptome analysis of cultured EPCs and MSCs indicated a trend toward higher expression levels of angiopoietin-1, hepatocyte growth factor, IGF-1, IGF-2, and VEGF-A in MSCs (which was not affected by GFP overexpression, data not shown), whereas platelet-derived growth factor-beta was predominantly expressed in EPCs (Table 1). Secretome analysis of conditioned medium from EPCs showed significantly higher levels of the pro-angiogenic protein PLGF ($p = 0.03$), whereas conditioned medium from MSCs contained higher VEGF and IGF-1 levels ($p \leq 0.05$) (Table 2).

Table 1 Transcriptional Analysis of EPC and MSC

	EPC $2^{-deltaCt}$ (n = 3)	MSC $2^{-deltaCt}$ (n = 3)	Mann-Whitney *U* Test
ANGPT-1	0.0004 (0.0002–0.02)	0.43 (0.14–0.64)	p = 0.1
ANGPT-2	2.45 (0.28–2.53)	0.23 (0.19–0.31)	p = 0.2
FGF-2	1.53 (0.39–7.81)	1.80 (0.17–2.16)	p = 1.0
HGF	0.001 (0.0005–0.02)	0.23 (0.13–0.39)	p = 0.1
HIF-1a	4.93 (3.22–12.77)	7.97 (4.87–10.09)	p = 1.0
IGF-1	0.04 (0.0005–0.08)	1.66 (0.12–2.20)	p = 0.1
IGF-2	0.002 (0–0.01)	0.77 (0.19–2.28)	p = 0.1
PDGF-a	0.018 (0.017–0.05)	0.03 (0.02–0.05)	p = 0.4
PDGF-b	1.24 (0.19–1.55)	0.0006 (0.0002–0.005)	p = 0.1
SDF-1	0.002 (0.00001–0.005)	0.03 (0.00001–0.11)	p = 0.4
TGF-β1	0.83 (0.62–2.81)	0.98 (0.41–1.25)	p = 1.0
VEGF-A	0.17 (0.06–0.42)	1.24 (1.06–1.70)	p = 0.1
VEGF-R2	0.25 (0.004–0.44)	0 (0–0.05)	p = 0.2

Values are presented as median (minimum to maximum); n indicates the number of cell cultures.
ANGPT = angiopoietin; EPC = endothelial progenitor cell; FGF = fibroblast growth factor; HGF = hepatocyte growth factor; HIF = hypoxia-inducible factor; IGF = insulin-like growth factor; MSC = mesenchymal stem cell; PDGF = platelet-derived growth factor; SDF = stromal cell derived factor; TGF = transforming growth factor; VEGF = vascular endothelial growth factor; VEGF-R = vascular enothelial growth factor receptor.

Hemodynamic and MRI measurements at 1 week and 7 weeks after AMI. HEMODYNAMIC MEASUREMENTS AND LABORATORY FINDINGS. Rate-pressure product 7 weeks after AMI did not differ between groups (7,689 ± 1,967 mm Hg/min; 6,441 ± 1,740 mm Hg/min; and 6,538 ± 1,087 mm Hg/min in CON [n = 12], EPC [n = 10], and MSC [n = 11]). No significant differences were observed in systolic or diastolic function at 7 weeks (dP/dt_{max}/IP: 30 ± 6 s^{-1} in CON, 33 ± 6 s^{-1} in EPC, 32 ± 6 s^{-1} in MSC; dP/dt_{min}: −1,554 ± 663 mm Hg/s in CON, −1,212 ± 386 mm Hg/s in EPC, −1,304 ± 266 mm Hg/s in MSC, p = NS for all).

On the basis of prior dose-finding studies, 34 ± 22 × 10^6 EPC and 10 ± 2 × 10^6 MSC were injected in the circumflex artery. Cell or placebo transfer was performed at 7 ± 1 days after AMI for all groups, and pigs were killed 6 weeks later. Hematological values and liver and renal function tests at 1 week and 7 weeks were within normal limits (data not shown).

CINE-ANGIOGRAPHY, DELAYED ENHANCEMENT, AND PERFUSION STUDIES USING MRI. In 2 pigs (both EPC), cineMRI could not be analyzed due to triggering artefacts. One week after AMI, LV ejection fraction equally and significantly decreased in all groups compared with values in healthy pigs. Six weeks later, ejection fraction showed a modest and similar increase in the 3 groups (Table 3); in contrast, LVESV significantly increased in CON and MSC but not in EPC (Online Fig. 1A, Table 3) ($p = 0.04$). A similar trend was measured for LVEDV (Online Fig. 1B, Table 3) ($p = 0.09$). Importantly, in 8 uninstrumented sham animals, body weight increased by 127% versus 90%, 100%, and 101% in infarcted CON, EPC, and MSC pigs, respectively. The concomitant,

Table 2 Secretome of EPC and MSC

	EPC (n = 4)	MSC (n = 4)	Mann-Whitney *U* Test
FGF-2 (pg/10^6)	17.0 (5.2–97.4)	7.1 (4.1–7.6)	p = 0.20
VEGF (pg/10^6)	29.4 (24.7–84.2)	424.1 (160.8–849.4)	p = 0.05
PLGF (pg/10^6)	732.5 (277.3–1214)	58.6 (33.8–87.9)	p = 0.03
IGF_1 (pg/10^6)	12.8 (8.9–49.5)	595.1 (125.6–997.6)	p = 0.02
$TGF\beta_1$ (pg/10^6)	44.0 (11.8–105.2)	54.1 (24.6–109.9)	p = 0.69

Values are presented as median (minimum to maximum); n indicates the number of experiments.
PLGF = placental growth factor; other abbreviations as in Table 1.

age-related increase in LVESV was 3 ± 8 ml/m^2 (+4%) in sham pigs but more than 2-fold higher after AMI in CON and MSC pigs (but not in EPC-treated pigs). Similarly, LVEDV increased by 15 ± 12 ml/m^2 with age in sham pigs (+26%), which again was further accentuated after AMI in CON and MSC but not in EPC pigs (+31% and +46% vs. +7%, respectively). Taken together, LV dilation in CON and MSC but not in EPC-treated pigs exceeds volume changes related to normal growth and aging.

No differences in initial infarct size were measured before cell transfer (Table 3), but the pattern of infarct remodeling was strikingly different, with a significant EPC treatment effect on infarct transmurality in the worst affected segments (overall p = 0.02 for segments with transmurality 50%, p = 0.005 for segments with transmurality 75%, and p = 0.003 for segments with 90% infarct transmurality) (Online Fig. 2). Myocardial perfusion, assessed in the area at risk (segments 5-6-11-12) during first-pass perfusion imaging, showed a trend for a greater relative upslope in EPC (72% [−2 to 119]) as compared with CON (25% [−33 to 236]) and MSC (−2% [−28 to 84]).

Histological analysis. PROGENITOR CELL ENGRAFTMENT/SURVIVAL. Immunohistochemical analysis with GFP antisera and confocal analysis to detect labeled MSCs in the infarcted heart (Fig. 3A) suggested the presence of GFP-positive cells in the infarct border zones These cells were also immunoreactive for desmin, as demonstrated on 5-μm adjacent sections (Figs. 3B and 3C). However, dual photon microscopy with spectral analysis failed to confirm the characteristic GFP emission spectrum at 509 nm in these areas (Figs. 3D to 3G), qPCR analysis failed to amplify GFP-transcripts in the border or infarct area from all 11 pigs, and immunoblot analysis with GFP-specific antisera did not reveal GFP immunoreactivity (data not shown). Prussian blue staining of sections from the infarct core and border zone of EPC-treated animals indicated focal areas with small vessels that contained feridex-labeled cells, which were immunoreactive for lectin (Figs. 3H to 3J). In the pigs who underwent cell transfer with LacZ-labeled EPC and MSC, LacZ histochemical staining of sections from the infarct core and border zone 6 weeks after cell transfer showed incorporation of labeled EPCs (Figs. 3K and 3L) but not MSCs. Labeled EPCs co-expressed von Willebrand factor (Fig. 3M) and were lining neovessels with smooth muscle actin-positive cells in the media (Fig. 3N), hence, they were capable of supporting blood flow. The qPCR analysis confirmed high LacZ transcript levels confined to the ischemic myocardium (data not shown). Histochemical analysis of labeled cells in remote organs did not find evidence for cell homing in other organs, other than for EPCs in splenic sinusoids, intersinusoidal red pulp around cords of Billroth, and endothelium of splenic venules (Figs. 4A and 4C). In the lung (Figs. 4E to 4H), LacZ expression was confined to the alveolar parenchyma of MSC-treated pigs (Fig. 4F). Taken together, these data suggest that allogeneic MSCs failed to permanently engraft, proliferate, or transdifferentiate in the ischemic territory after IC injection 6 weeks after AMI, whereas late-outgrowth EPCs participate in neovascularization.

VASCULAR DENSITY IN INFARCT CORE AND BORDER ZONE. To evaluate whether changes in infarct remodeling and perfusion were associated with enhanced neovascularization, vascular density was determined on lectin-stained sections from the infarct core, border zone, and remote myocardium (Fig. 5). No differences were seen between groups in the infarct core or remote myocardium. However, in the border zone, vascular density was significantly higher in EPC rather than in CON and MSC (p = 0.01). Representative examples from the infarct border zone of CON, EPC, and MSC show 15%, 34%, and 20% capillaries over total number of cells/high-power field, respectively. Interestingly, a trend toward higher expression levels of the anti-apoptotic BCL-XL gene was seen in EPC rather than in CON and MSC, most likely attrib-

Table 3 MRI Data at 1 Week and 7 Weeks After AMI

	CON (n = 7)			EPC (n = 7)			MSC (n = 7)			
	Week 1	Week 7	Change	Week 1	Week 7	Change	Week 1	Week 7	Change	p Value
$LVEDV_i$ (ml/m^2)	64 ± 19	81 ± 17	17 ± 12	74 ± 20	76 ± 24	2 ± 18	65 ± 20	85 ± 22	20 ± 15	0.09
$LVESV_i$ (ml/m^2)	35 ± 13	42 ± 14	7 ± 8	43 ± 16	40 ± 16	−3 ± 11	37 ± 12	48 ± 16	11 ± 12	0.04
EF (%)	46 ± 8	48 ± 7	3 ± 6	44 ± 10	49 ± 8	5 ± 11	44 ± 5	45 ± 7	2 ± 11	0.64
				EPC (n = 9)						
Infarct size (%)	15 ± 4	9 ± 4	−6 ± 4	17 ± 7	9 ± 5	−8 ± 8	16 ± 9	7 ± 1	−8 ± 9	0.84

Infarct size is expressed as percentage of total myocardial mass. Values are presented as mean ± SD; p values indicate differences among 3 groups (Kruskal-Wallis).
AMI = acute myocardial infarction; EF = ejection fraction; LVEDV = left ventricular end-diastolic volume; LVESV = left ventricular end-systolic volume; MRI = magnetic resonance imaging; other abbreviations as in Table 1.

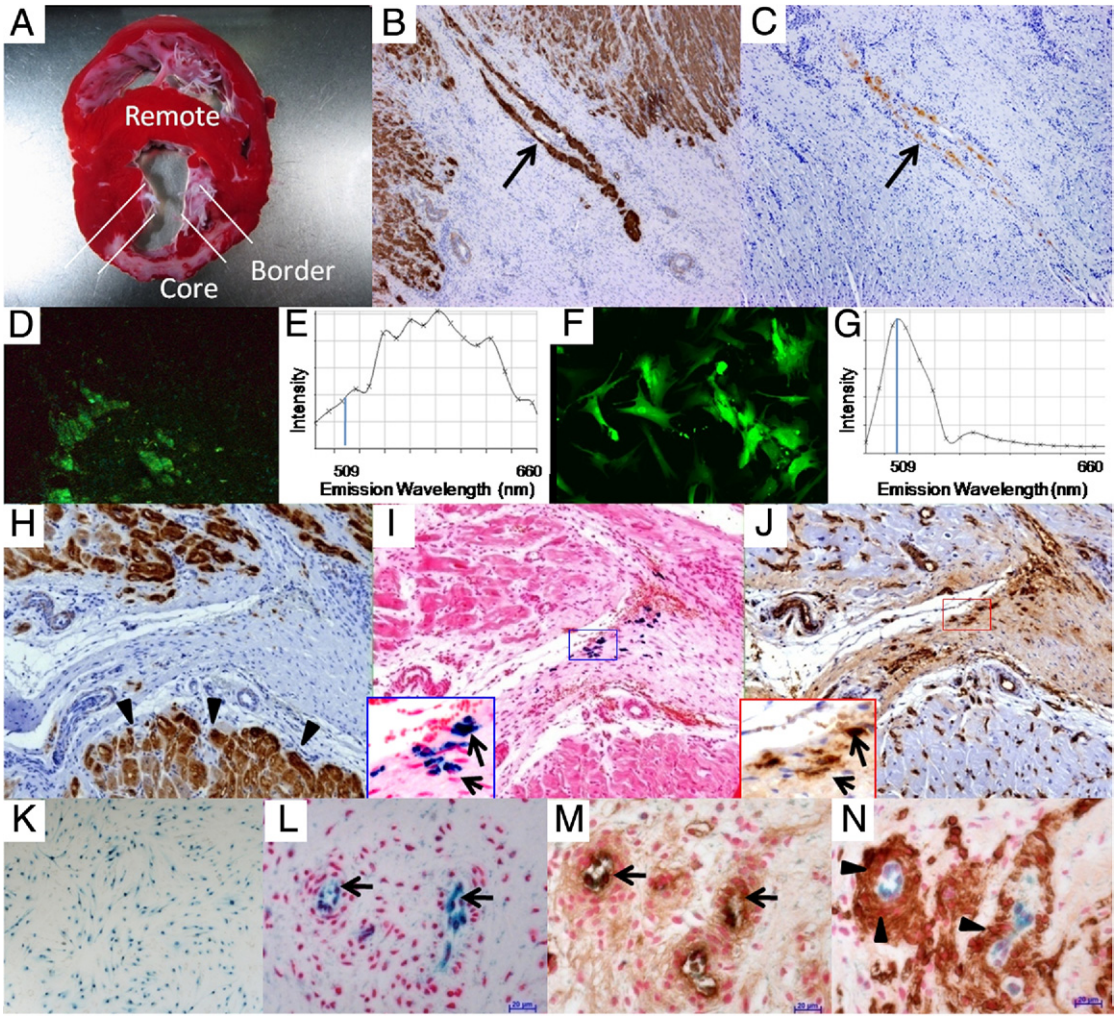

Figure 3 **Histological Analysis of Progenitor Cell Engraftment in the Infarcted Myocardium**

At 7 weeks, transverse sections of the heart stained with 2,3,5-triphenyltetrazoliumchloride show infarct core, border zone, and remote area **(A)**. Immunohistochemical staining with desmin **(B)** and green fluorescent peptide (GFP) antisera **(C)** in border zone of pigs treated with enhanced GFP-transduced MSCs. The GFP-positive cells were also immunoreactive for desmin, as demonstrated on 5-μm adjacent sections **(arrows)**. Dual photon laser microscopy **(D)** with spectral analysis **(E)** failed to show the characteristic 509-nm GFP-emission amplitude in myocardial tissue sections, whereas the characteristic GFP emission wavelength was clearly present in lenti-GFP infected bone marrow cells (positive controls) **(F, G)**. Prussian blue staining of sections from infarct border zone **(arrowheads)** of EPC **(H)** (desmin staining) showed focal areas of small vessels containing Endorem-labeled cells **(arrows, I)**, which are reactive to lectin staining on 5-μm adjacent sections **(arrows, J)**. Six weeks after cell transfer of beta-galactosidase–labeled EPCs **(K)**, beta-galactosidase histochemical staining of sections from the infarct border zone showed incorporation in neovessels **(arrows, L)**, which were also immunoreactive for von Willebrand factor **(arrows, M)** and smooth muscle actin in the media **(arrowheads, N)**. Abbreviations as in Figure 1.

utable to paracrine trophic effects of EPCs on cardiomyocytes at risk in the border zone (Online Table 2).

EXTRACELLULAR MATRIX DEGRADATION AND VENTRICULAR REMODELING. Infarct patterns are shown on representative TTC stains from the 3 groups (Figs. 6A to 6C). Quantitative PCR analysis in the infarct border zone showed that matrix metalloproteinase (MMP)-2 is the most abundantly expressed metalloproteinase in the infarcted porcine heart. Its expression was significantly reduced in EPC-treated pigs compared with MSC and CON (Online Fig. 3). Transcript levels of the other MMPs and thrombospondin-1 did not differ between groups. These findings were associated with less-pronounced MMP-2 immunoreactivity in the infarct border zone of EPC-treated pigs (Figs. 6D to 6F). Sirius red staining (Figs. 6G to 6I) and polarized light microscopy of the infarct border zone (Figs. 6J to 6L) showed a better organized scar in EPC than in CON and MSC. Finally, a trend toward reduced porcine brain natriuretic peptide and porcine atrial natriuretic peptide transcript levels in the infarct border zone was detected in EPC-treated animals, consistent with the observed changes in remodeling (Online Table 2).

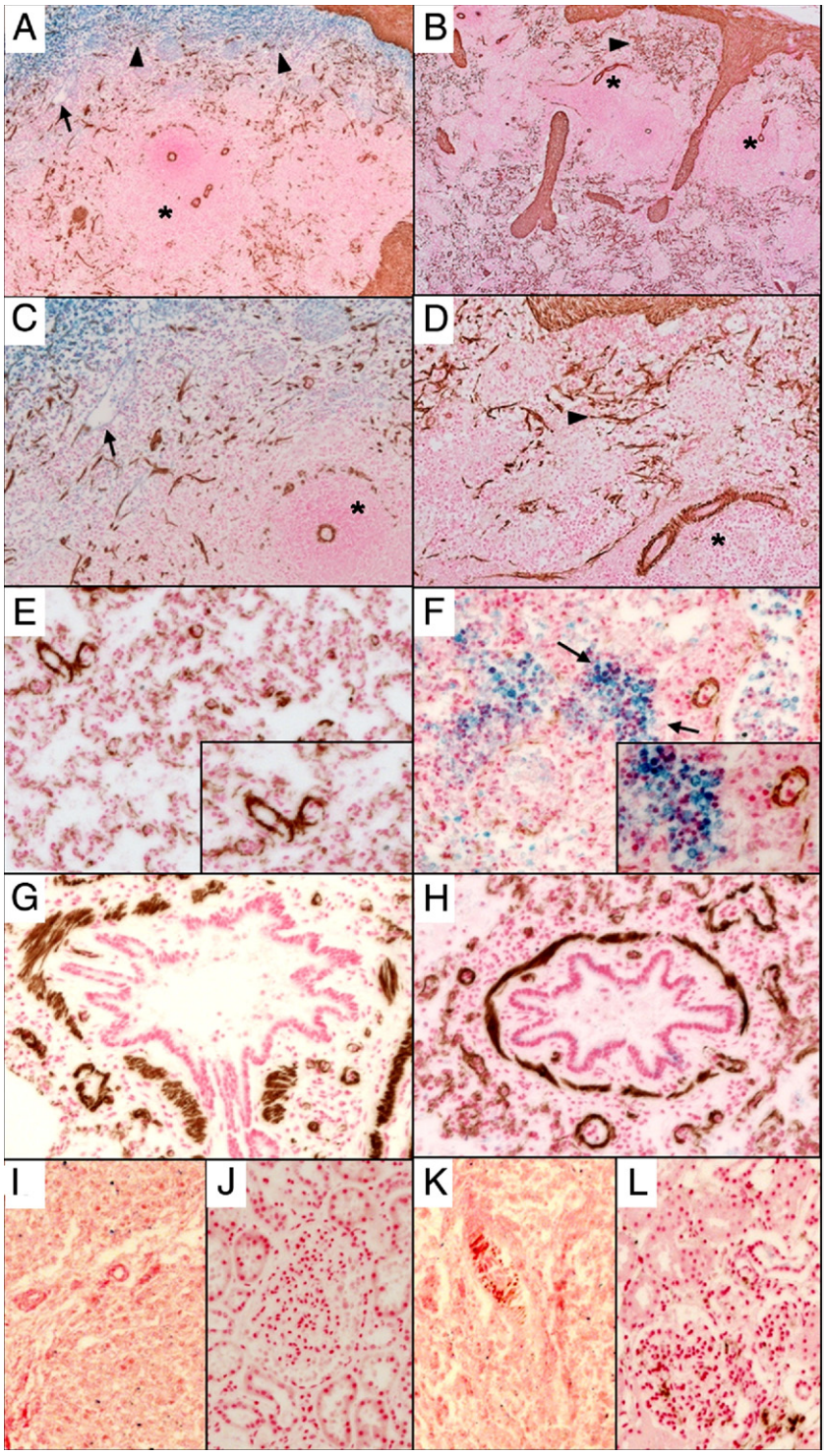

Figure 4 **Biodistribution of Labeled MSC and EPCs After Intracoronary Injection**

Localization of beta-galactosidase (LacZ) labeled **(blue)** EPCs **(A, C, E, G, I, J)** and MSCs **(B, D, F, H, K, L)** in extracardiac tissues 1 week after delivery. After LacZ staining, histologic sections were stained with alpha-smooth muscle actin antisera **(brown)** and counterstained with nuclear fast red. In the spleen **(A to D)**, strong LacZ expression was confined to the sinusoids **(arrowheads)**, intersinusoidal red pulp around cords of Billroth, and endothelium of venules **(arrows)** in EPC-treated pigs. The LacZ expression was absent in splenic arterioles and surrounding lymphoid white pulp **(asterisks)** or trabecular meshwork **(brown)** of EPC- and MSC-treated pigs. In lungs **(E to H)**, LacZ expression was only detected in alveolar parenchyma of MSC-treated pigs **(F, arrows and inset)** but not in EPC pigs **(E)**. No LacZ expression was detected in bronchioles or peri-bronchiolar lung tissue **(G, H)**, liver **(I, K)**, or kidney **(J, L)**. Abbreviations as in Figure 1.

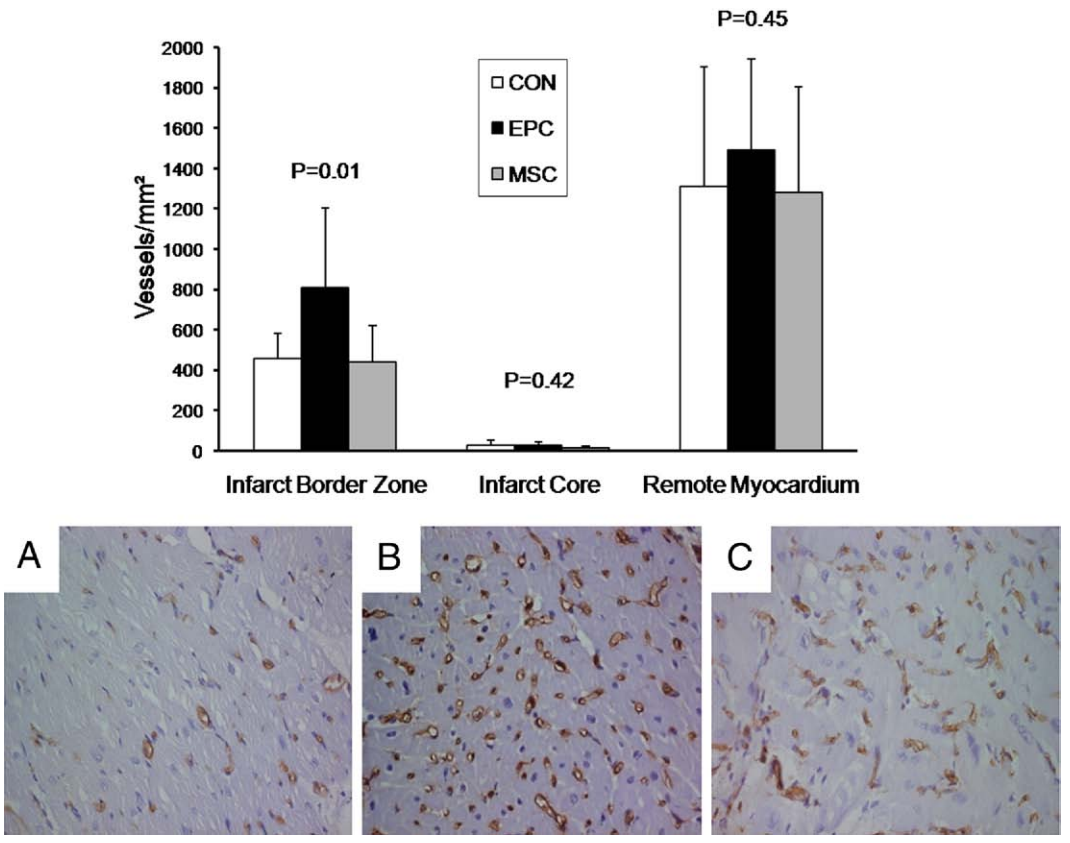

Figure 5 Vascular Density in Infarct Border, Infarct Core, and Remote Myocardium

(Top) vascular density was similar between groups in the infarct core or remote myocardium but significantly higher in the border zone of EPC compared with CON and MSC ($p = 0.01$). **(Bottom)** representative lectin-stained sections from the infarct border zone of CON **(A)**, EPC **(B)**, and MSC **(C)**. Abbreviations as in Figure 1.

Discussion

In this study we report that IC infusion of autologous late-outgrowth EPCs 1 week after AMI does not enhance LV global function recovery but prevents LV volume expansion as measured by MRI at 7-week follow-up. In pigs randomized to allogeneic MSCs or CON, LV remodeling after myocardial infarction was characterized by marked ESV and EDV expansion (Online Fig. 1, Table 3), which exceeded natural growth-related increase greater than 2-fold over the same period. Transfer of late-outgrowth EPCs was associated with better infarct remodeling, as evidenced by smaller transmural extent of delayed enhancement in most severely affected myocardial segments (Online Fig. 2) and by significantly greater vascular density (Fig. 5) and a trend toward enhanced anti-apoptotic gene expression and reduced natriuretic peptide expression in the infarct border zone. Postmortem dual photon microscopic analysis failed to provide evidence for progenitor cell-mediated cardiomyogenesis, but confocal analysis clearly demonstrated incorporation of genetically labeled EPCs in muscularized neovessels in the infarct border zone (Fig. 3). Gene expression and protein release profiles of cultured progenitor cell populations are consistent with a greater neovascularization potential of autologous late-outgrowth EPCs compared with allogeneic MSCs and might hold promise for novel cell-based strategies to target post-infarction heart failure.

We compared functional repair capacity of 2 selected well-characterized progenitor cell populations in a representative large animal model of ischemic cardiomyopathy. To distinguish autocrine versus paracrine effects of infused cells, we used robust molecular labeling strategies in combination with dual photon laser microscopy of the infarct core and border zones. We did not detect engrafted or transdifferentiated MSCs 6 weeks after injection in the IRA, consistent with recent reports from several laboratories that have suggested indirect vasculogenic effects or stimulatory effects on endogenous resident stem cells (17–19). Loss of plasticity of infused allogeneic MSCs after lentiviral infection or multiple in vitro passages or impaired growth factor synthesis capacity is unlikely, as evidenced in osteogenic and adipogenic differentiation assays and secretome analysis. However, alternative cell delivery methods, including intramyocardial injection of MSC or cardiomyogenic pre-

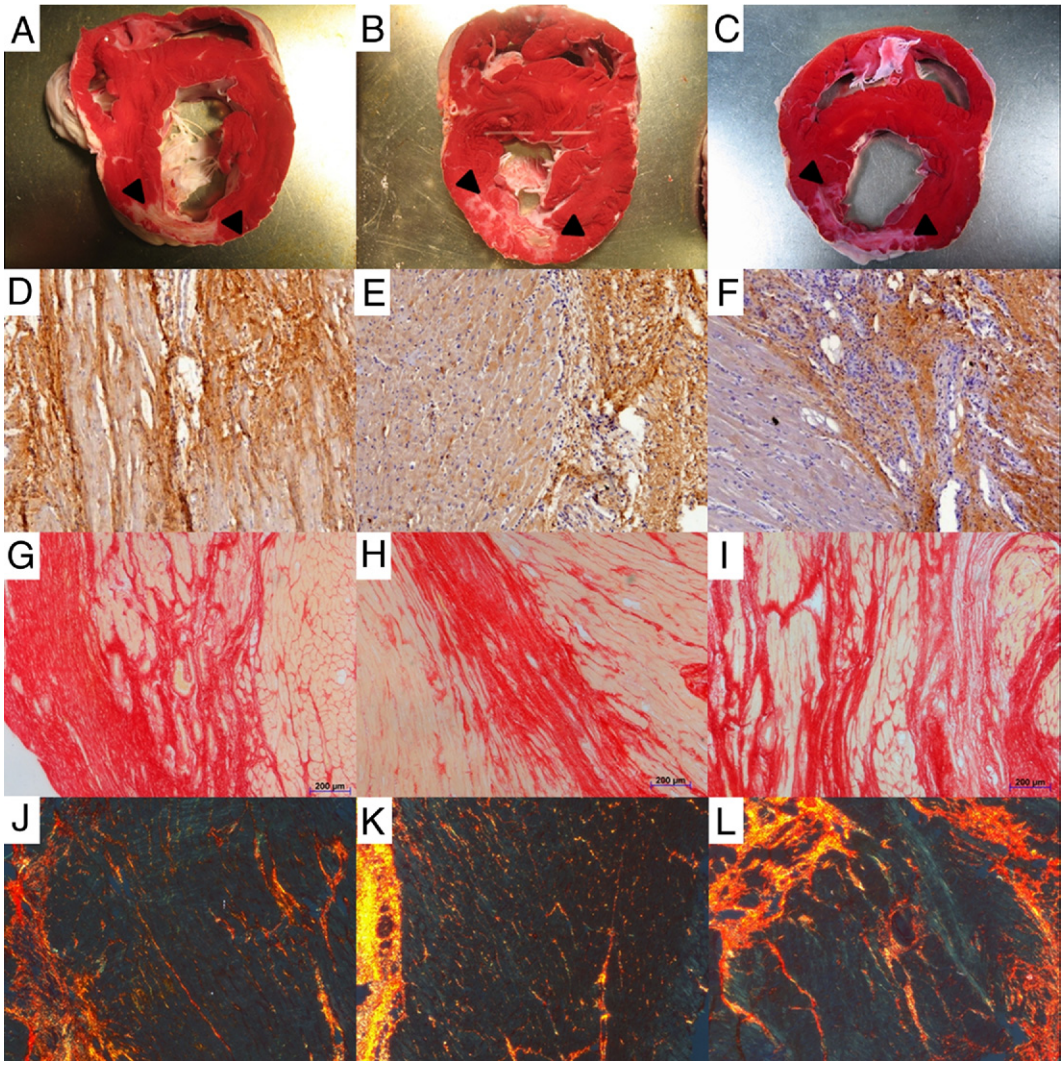

Figure 6 **MMP2 Expression and Collagen Deposition in Infarct Border**

Infarct borders were identified on representative examples of 2,3,5-triphenyltetrazoliumchloride stains in CON, EPC, and MSC **(A to C, arrowheads)**. In the border zone of EPC **(E)**, matrix metalloproteinase (MMP)-2 immunoreactivity was less pronounced as compared with CON **(D)** and MSC **(F)**. After Sirius red staining **(G to I)**, polarized light microscopy **(J to L)** suggested a better organized fibrous scar in EPC **(K)** than in CON **(J)** and MSC **(L)**. Other abbreviations as in Figure 1.

specification of MSCs before in vivo transfer, might enhance their biological repair capacity (20). Of note, we observed that IC infusion of 10×10^6 MSC was associated with a transient reduction in epicardial coronary flow, as measured by MRI, precluding IC injection of higher doses and suggesting that direct intramyocardial injection might be preferable for larger progenitor cells. A similar impediment in epicardial coronary flow was recently reported in an open chest swine model with online near-infrared imaging (21). In contrast, 6 weeks after EPC transfer we observed focal areas containing Prussian blue-stained cells lining small vessels in the infarct border zone (Fig. 3), suggesting partial engraftment and survival of EPCs in the border zone. Endorem labeling does not affect tube formation capacity of late outgrowth EPCs on matrigel (data not shown) but precludes accurate evaluation of in vivo engraftment efficiency, because labeling will be lost upon cell turnover. Therefore, robust genetic labeling with lentiviral LacZ constructs provided proof of concept that transferred late-outgrowth EPCs integrate into new blood vessels.

Because most recent cell-based clinical studies suggest paracrine trophic mechanisms for the observed changes in infarct remodeling or functional recovery (2–4,22,23), we investigated the transcriptome and secretome of both progenitor cell populations. Limited availability of porcine-specific gene sequences and commercial antibodies precluded an in-depth analysis of all growth factors operational in humans. We observed a trend for higher platelet-derived growth factor-b transcript levels in EPCs as well as a trend

for higher angiopoietin-1, hepatocyte growth factor, IGF-1, IGF-2, and VEGF-A transcript levels in MSCs. Of interest, levels of the pro-angiogenic protein PLGF were significantly and consistently higher in conditioned medium from EPCs compared with MSCs. The latter, in contrast, released more VEGF and IGF-1, which also play a role in angiogenic differentiation pathways. Although protein- and gene-based VEGF administration has failed to induce therapeutic neovascularization in controlled clinical trials, PLFG has recently been shown to enhance post-infarction myocardial repair and collateral flow development via arteriogenesis (24,25). The greater neovascularization potential of EPCs in our study was evidenced by a greater vascular density in the infarct border zone (Fig. 5) and by a trend for enhanced myocardial perfusion after MRI contrast injection. The extent to which greater release of PLGF from late outgrowth EPCs is responsible for the observed biological effects needs to be determined in specifically designed follow-up studies and has significant therapeutic implications (26).

The observed changes in LV remodeling in EPC-treated pigs suggest that not only absolute infarct size but, more importantly, the pattern of infarct healing might be clinically relevant. Recent clinical MRI studies have also clearly demonstrated that reduction in infarct transmurality over time determines LV adverse remodeling, development of heart failure, and clinical outcome (27). Animals treated with EPCs develop less thinning of infarcted myocardial segments, most likely because of enhanced perfusion and reduced apoptosis in the infarct border zone, causing less myocardial strain and infarct expansion. Finally, less LV expansion over time in EPC-treated animals was also consistent with a better-organized fibrous scar (Fig. 6) and with reduced MMP2 expression in the infarct border (Online Fig. 3).

Study limitations. We recognize the limitations of replicating clinical conditions in a relatively small set of animals. Although we made every effort to use identical cell transfer and imaging methodologies as in clinical studies and included age-matched control pigs treated with IC placebo injection and a separate series of uninfarcted pigs to account for growth-related volume changes, the remodeling data were obtained after 6 weeks in the absence of beta-blocker or angiotensin-converting enzyme inhibitor therapy in a nonatherosclerotic background. Also, we only studied a single dose of EPCs and MSCs, which were, however, previously determined to be safe and well-tolerated (data not shown). Higher doses of MSCs caused intravascular obstruction (X. Liu, unpublished observations, June 2007). Importantly, we cannot exclude different results after direct intramyocardial injection of MSCs, as demonstrated in previous porcine studies (28,29). We are unable to compare our results with selected CD34+-hematopoietic cells, in the absence of available selection markers. Finally, follow-up was limited to 6 weeks after cell transfer, because excessive weight gain precludes MRI analysis thereafter. Therefore, we cannot determine whether or not observed benefits in LV remodeling mitigate development of overt heart failure and increase long-term survival.

Conclusions

IC transfer of selected progenitor cell populations does not lead to long-term stable transdifferentiation into competent cardiomyocytes. Infusion of late-outgrowth EPCs after AMI is feasible and safe and limits maladaptive LV remodeling via autocrine and paracrine pro-angiogenic effects. Late-outgrowth EPC transfer might hold promise for heart failure treatment in patients with ischemic cardiomyopathy.

Reprint requests and correspondence: Dr. Stefan Janssens, Division of Clinical of Cardiology and Vesalius Research Center, Campus Gasthuisberg, University of Leuven, 49 Herestraat, B-3000 Leuven, Belgium. E-mail: stefan.janssens@med.kuleuven.be.

REFERENCES

1. Orlic D, Kajstura J, Chimenti S, et al. Bone marrow cells regenerate infarcted myocardium. Nature 2001;410:701–5.
2. Janssens S, Dubois C, Bogaert J, et al. Autologous bone marrow-derived stem-cell transfer in patients with ST-segment elevation myocardial infarction: double-blind, randomised controlled trial. Lancet 2006;367:113–21.
3. Lunde K, Solheim S, Aakhus S, et al. Intracoronary injection of mononuclear bone marrow cells in acute myocardial infarction. N Engl J Med 2006;355:1199–209.
4. Schachinger V, Erbs S, Elsasser A, et al. Intracoronary bone marrow-derived progenitor cells in acute myocardial infarction. N Engl J Med 2006;355:1210–21.
5. Dimmeler S, Burchfield J, Zeiher AM. Cell-based therapy of myocardial infarction. Arterioscler Thromb Vasc Biol 2008;28:208–16.
6. Freyman T, Polin G, Osman H, et al. A quantitative, randomized study evaluating three methods of mesenchymal stem cell delivery following myocardial infarction. Eur Heart J 2006;27:1114–22.
7. Grogaard HK, Sigurjonsson OE, Brekke M, et al. Cardiac accumulation of bone marrow mononuclear progenitor cells after intracoronary or intravenous injection in pigs subjected to acute myocardial infarction with subsequent reperfusion. Cardiovasc Revasc Med 2007;8:21–7.
8. Hansen A, Wolf D, Reinhard A, Katus HA, Kuecherer H, Hansen A. Dose-dependent effects of intravenous allogeneic mesenchymal stem cells in the infarcted porcine heart. Stem Cells Dev 2009;18:321–9.
9. Hashemi SM, Ghods S, Kolodgie FD, et al. A placebo controlled, dose-ranging, safety study of allogenic mesenchymal stem cells injected by endomyocardial delivery after an acute myocardial infarction. Eur Heart J 2008;29:251–9.
10. Hou D, Youssef EA, Brinton TJ, et al. Radiolabeled cell distribution after intramyocardial, intracoronary, and interstitial retrograde coronary venous delivery: implications for current clinical trials. Circulation 2005;112:I150–6.
11. Pittenger MF, Mackay AM, Beck SC, et al. Multilineage potential of adult human mesenchymal stem cells. Science 1999;284:143–7.
12. Pittenger MF, Martin BJ. Mesenchymal stem cells and their potential as cardiac therapeutics. Circ Res 2004;95:9–20.
13. Cerqueira MD, Weissman NJ, Dilsizian V, et al. Standardized myocardial segmentation and nomenclature for tomographic imaging of the heart: a statement for healthcare professionals from the Cardiac Imaging Committee of the Council on Clinical Cardiology of the American Heart Association. Circulation 2002;105:539–42.
14. Kim RJ, Wu E, Rafael A, et al. The use of contrast-enhanced magnetic resonance imaging to identify reversible myocardial dysfunction. N Engl J Med 2000;343:1445–53.

15. Barkhausen J, Hunold P, Jochims M, Debatin JF. Imaging of myocardial perfusion with magnetic resonance. J Magn Reson Imaging 2004;19:750–7.
16. Nagel E, Klein C, Paetsch I, et al. Magnetic resonance perfusion measurements for the noninvasive detection of coronary artery disease. Circulation 2003;108:432–7.
17. de Silva R, Raval AN, Hadi M, et al. Intracoronary infusion of autologous mononuclear cells from bone marrow or granulocyte colony-stimulating factor-mobilized apheresis product might not improve remodeling, contractile function, perfusion, or infarct size in a swine model of large myocardial infarction. Eur Heart J 2008;29:1772–82.
18. Ramos GA, Hare JM. Cardiac cell-based therapy: cell types and mechanisms of actions. Cell Transplant 2007;16:951–61.
19. Mazhari R, Hare JM. Mechanisms of action of mesenchymal stem cells in cardiac repair: potential influences on the cardiac stem cell niche. Nat Clin Pract Cardiovasc Med 2007;4 Suppl 1:S21–6.
20. Bartunek J, Croissant JD, Wijns W, et al. Pretreatment of adult bone marrow mesenchymal stem cells with cardiomyogenic growth factors and repair of the chronically infarcted myocardium. Am J Physiol Heart Circ Physiol 2007;292:H1095–104.
21. Ly HQ, Hoshino K, Pomerantseva I, et al. In vivo myocardial distribution of multipotent progenitor cells following intracoronary delivery in a swine model of myocardial infarction. Eur Heart J 2009;30:2861–8.
22. Huikuri HV, Kervinen K, Niemela M, et al. Effects of intracoronary injection of mononuclear bone marrow cells on left ventricular function, arrhythmia risk profile, and restenosis after thrombolytic therapy of acute myocardial infarction. Eur Heart J 2008;29:2723–32.
23. Tendera M, Wojakowski W, Ruzyllo W, et al. Intracoronary infusion of bone marrow-derived selected CD34+CXCR4+ cells and nonselected mononuclear cells in patients with acute STEMI and reduced left ventricular ejection fraction: results of randomized, multicentre Myocardial Regeneration by Intracoronary Infusion of Selected Population of Stem Cells in Acute Myocardial Infarction (REGENT) Trial. Eur Heart J 2009;30:1313–21.
24. Pipp F, Heil M, Issbrucker K, et al. VEGFR-1-selective VEGF homologue PlGF is arteriogenic: evidence for a monocyte-mediated mechanism. Circ Res 2003;92:378–85.
25. Roncal C, Buysschaert I, Chorianopoulos E, et al. Beneficial effects of prolonged systemic administration of PlGF on late outcome of post-ischaemic myocardial performance. J Pathol 2008;216:236–44.
26. Marsboom G, Janssens S. Endothelial progenitor cells: new perspectives and applications in cardiovascular therapies. Expert Rev Cardiovasc Ther 2008;6:687–701.
27. Bogaert J, Kalantzi M, Rademakers FE, Dymarkowski S, Janssens S. Determinants and impact of microvascular obstruction in successfully reperfused ST-segment elevation myocardial infarction. Assessment by magnetic resonance imaging. Eur Radiol 2007;17:2572–80.
28. Amado LC, Saliaris AP, Schuleri KH, et al. Cardiac repair with intramyocardial injection of allogeneic mesenchymal stem cells after myocardial infarction. Proc Natl Acad Sci U S A 2005;102:11474–9.
29. Schuleri KH, Amado LC, Boyle AJ, et al. Early improvement in cardiac tissue perfusion due to mesenchymal stem cells. Am J Physiol Heart Circ Physiol 2008;294:H2002–11.

Key Words: cell therapy ■ endothelial progenitor cells ■ left ventricular remodeling ■ mesenchymal stem cells ■ myocardial infarction.

APPENDIX

For supplementary tables and a supplemental figure, please see the online version of this article.